

## **Supplemental Methods and Supplemental Data Figures 1-9 for Li et al. “Graft IL-33 regulates infiltrating macrophages to protect against chronic rejection”**

### **Supplemental Methods:**

#### **Quantitative Immunofluorescence.**

Mouse HTx or naïve heart sections were stained following protocols established in the Center for Biologic Imaging, University of Pittsburgh (<http://cbi.pitt.edu>) as previously described (1). Primary antibodies to CD45 (BD Biosciences, Rat anti-mouse, 550539), vimentin (Abcam, chicken anti-mouse, ab73159), and IL-33 (R&D systems, goat anti-mouse, AF3626) were followed by secondary antibodies conjugated to Alexa Fluor 488 (Donkey anti-Goat IgG, Invitrogen, A1105), Cy3 (Donkey anti-Rat IgG, Jackson, 712-1665-153) or Cy5 (Donkey anti-chicken, Jackson, 703-175-155). Nuclei were stained with 4',6-diamidino-2-phenylindole (DAPI; Sigma). Sections were visualized on a Nikon A1 Spectral Confocal microscope and analyzed using Nikon NIS Elements Software.

IL-33 staining of paraffin-embedded EMB from pediatric heart transplant recipients was completed following sectioning, deparaffinization, and antigen retrieval (pH 9.0; 30-40 minutes) and using a rabbit anti-human IL-33 antibody (R&D, MAB36252) or a rat anti-IL-33 antibody (R&D, 390412) and anti-rat or -rabbit biotinylated IgG secondary antibodies (Vector Labs), and streptavidin-conjugated Qdot 655 or Dylight 650. Pixel-based image analytics were completed using NearCYTE for quantitation of fluorescent emissions following whole slide image capture with a Zeiss Axio Scan Z.1 scanner utilizing a with a 16-bit color sCMOS camera (Hamamatsu Photonics), and HXP-120V metal halide excitation source or monochrome camera, and appropriate filters.

Intra-graft macrophage immunolabeling was completed on paraffin-embedded sections placed on glass slides. Sections were deparaffinized and antigens were retrieved using 10 mM citrate antigen retrieval buffer (pH=6), and background fluorescence was quenched using a copper sulfate solution (10mM CuSO<sub>4</sub>, 50 mM ammonium acetate, pH 5.0). Sections were then blocked for 1h at room temperature with a solution consisting of 0.1% Triton-X100, 0.1% Tween 20, 5% normal goat serum, and 2% BSA. A rabbit anti-CD11b (Abcam, ab128797) antibody was then applied overnight in a humidified chamber at 4°C. Following overnight incubation, sections were washed with Tris/Tween 20 buffered saline (TBST) and incubated with goat-anti-rabbit (DAKO, P0448) HRP-conjugated secondary antibody and then microwaved at 40% power for 3 minutes. Sections were subsequently washed with TBST and incubated for 10 minutes in the dark with Opal Polaris 570 reagent (Akoya, FP1488001KT). Slides were then washed in TBST, and antigen retrieval and blocking were again performed as described above. This was followed by incubation overnight at 4°C with a rabbit anti-iNOS (Thermo Fisher, PA0303A) antibody. Sections were washed with TBST, secondary antibody was applied as specified above, and Opal Polaris 470 reagent (Akoya, FP1500001KT) was applied for 10 minutes in the dark. Sections were then washed, nuclei were counterstained with DAPI for 5 minutes, and given a final washed with TBST prior to coverslip mounting. Three to five randomly 20x selected images were acquired per recipient using an inverted fluorescence microscope (Axio Observer Z1, Carl Zeiss) and images were quantified using CellProfiler (<https://cellprofiler.org>).

#### **Cellular mitochondrial bioenergetics assay of BMDM.**

Mitochondrial bioenergetics/function was assessed using Seahorse XF96e Analyzer (Agilent Technologies, Santa Clara, CA). BMDM generated as described in the *Materials and Methods* and 1x10<sup>5</sup> per well were seeded on Cell-Tak coated Seahorse 96 well plate and cultured for 15-18h in complete media alone (M0) or media supplemented with 20 ng/mL IFN<sub>γ</sub> (Affymetrix

eBioscience) and 100 ng/mL LPS (Sigma Aldrich), 20 ng/mL IL-4 (Invitrogen), or 20 ng/ml IL-33 (Peprotech). After the incubation the media was removed and the cells were equilibrated in Seahorse XF media at 37°C for one hour prior to measuring the mitochondrial oxygen consumption rate (OCR) and extracellular acidification rate (ECAR). The mitochondrial stress was carried out as described previously (2). OCR and ECAR were measured in response to the addition of 1  $\mu$ M oligomycin, 1.5  $\mu$ M fluoro-carbonyl cyanide phenylhydrazone (FCCP), and 0.1  $\mu$ M rotenone plus 1  $\mu$ M antimycin A.

## **Untargeted Metabolomic Analysis of BMDM.**

### **BMDM sample preparation**

BMDM were generated described in the *Materials and Methods* and cultured at  $2 \times 10^6$  cell per well in a 6-well plate for 15 h in complete media alone (M0) or media supplemented with one or combinations of the following: 1) 20 ng/mL IFN $\gamma$  (Affymetrix eBioscience) and 100 ng/mL LPS (Sigma Aldrich); 2) 20 ng/mL IL-4 (Invitrogen); 3) 20 ng/ml IL-33 (Peprotech). After the incubation period of at 37°C and 5% CO $_2$ , cells were washed with sterile PBS and metabolic quenching and polar metabolite pool extraction was performed using ice cold 80% methanol / 0.1% formic acid at a ratio of 500 $\mu$ L per  $1 \times 10^6$  cells. An internal standard mix that included deuterated (D $_3$ )-creatinine, (D $_3$ )-alanine, (D $_4$ )-taurine and (D $_3$ )-lactate (Sigma-Aldrich) was added to the sample lysates at a final concentration of 10 $\mu$ M. After 3 minutes of vortexing, the supernatant was cleared of protein by centrifugation at 16,000xg. Cleared supernatant (3  $\mu$ L) was subjected to online LC-HRMS analysis using an incomplete block design sequence.

### **LC-HRMS Method**

Briefly, samples were injected via a Thermo Vanquish ultra-high performance liquid chromatography (UHPLC) and separated over a reversed phase Thermo HyperCarb porous graphite column (2.1 $\times$ 100 mm, 3  $\mu$ m particle size) maintained at 55°C. For the 20 minute LC gradient, the mobile phase consisted of the following: solvent A (water/0.1% FA) and solvent B (ACN/0.1% FA). The gradient was the following: 0-1 min 1%B, increasing to 15%B over 5 min, and then to 98%B over five minutes followed by a hold at 98%B for five minutes, and equilibration to starting conditions at 1%B for 5 min. The Thermo ID-X tribrid mass spectrometer was operated in both positive and negative ion mode, scanning in Full MS mode (2  $\mu$ scans) from 100 to 800  $m/z$  at 70,000 resolution with an AGC target of  $2 \times 10^5$ . Source ionization setting was +3.0 kV or -2.7kV spray voltage for positive and negative mode, respectively. Source gas parameters were 35 sheath gas, 12 auxiliary gas at 320°C, and 8 sweep gas. Calibration was performed prior to analysis using the Pierce<sup>TM</sup> FlexMix Ion Calibration Solutions (Thermo Fisher Scientific). For specific analytes, integrated peak areas were extracted manually using Quan Browser (Thermo Fisher Xcalibur ver. 2.7). Mass tolerances used for database matching was 5 ppm for full scan and 0.5 Da for MS/MS fragments. All analyte peak areas were normalized to internal standard and cell number.

### **Electron paramagnetic resonance (EPR) spectroscopy and spin trapping of NO released from BMDM.**

BMDM generated as described in the *Materials and Methods* and  $1 \times 10^5$  cells/well were seeded in a 96-well plate and cultured for 15 h in complete media alone (M0) or media supplemented with 20 ng/mL IFN $\gamma$  (Affymetrix eBioscience) and 100 ng/mL LPS (Sigma Aldrich), 20 ng/mL IL-4 (Invitrogen), or 20 ng/ml IL-33 (Peprotech). After the incubation the cells were washed one time with PBS (without CaCl $_2$  and MgCl $_2$ ) and medium containing the Fe(MGD) $_2$  complexes and 0.1 mM of L-Arginine was added. Cells were incubated at 37°C, 5% CO $_2$  for 20 minutes and the

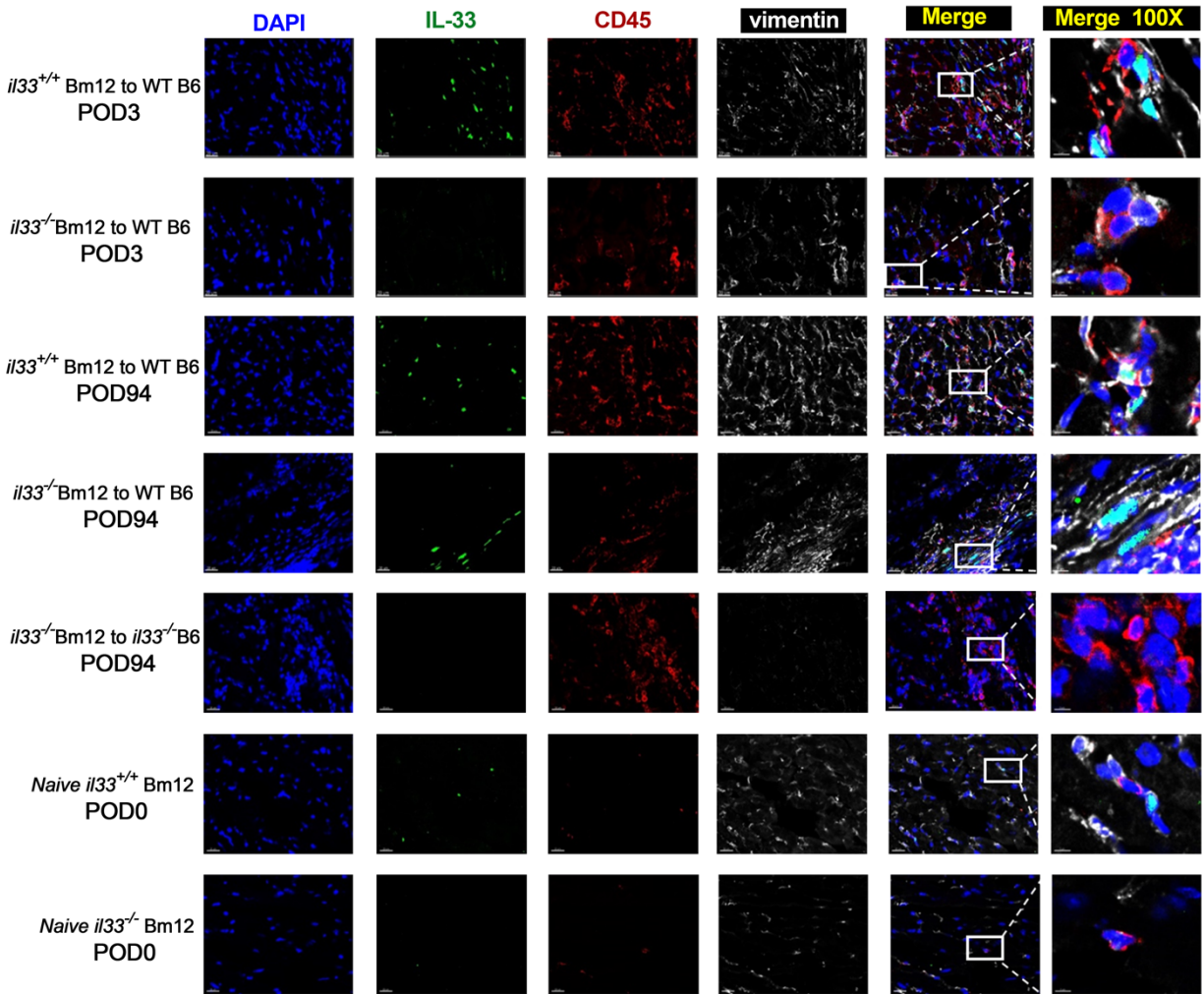
supernatant was collected and immediately frozen in liquid nitrogen. Supernatants were stored at -80°C until the EPR experiments were carried out. X-band EPR spectra were recorded on a Bruker EMX premiumX spectrometer equipped with HQ cavity. The liquid samples (50 µL) were loaded in a glass capillary tube and one end was closed using Critoseal clay. EPR measurements were performed at ambient temperature as previously described (3). The EPR instrument parameters used were as follows: microwave frequency, 9.85 GHz; sweep width, 70 G; receiver gain, 30 dB; modulation amplitude, 5 G; microwave power, 40 mW; conversion time, 17.86 ms, time constant, 5.12 ms, scan time, 20 s; number of scans, 30. Spin-trapping measurements of NO were performed using Fe(MGD)<sub>2</sub> complex as the spin trap (4, 5). The Fe(MGD)<sub>2</sub> complex (0.5 mM Fe<sup>2+</sup> and 10 mM MGD) was used to trap the NO generated in BMDM cultures.

### **Quantitative real time PCR (qRT-PCR) analysis of immune cells.**

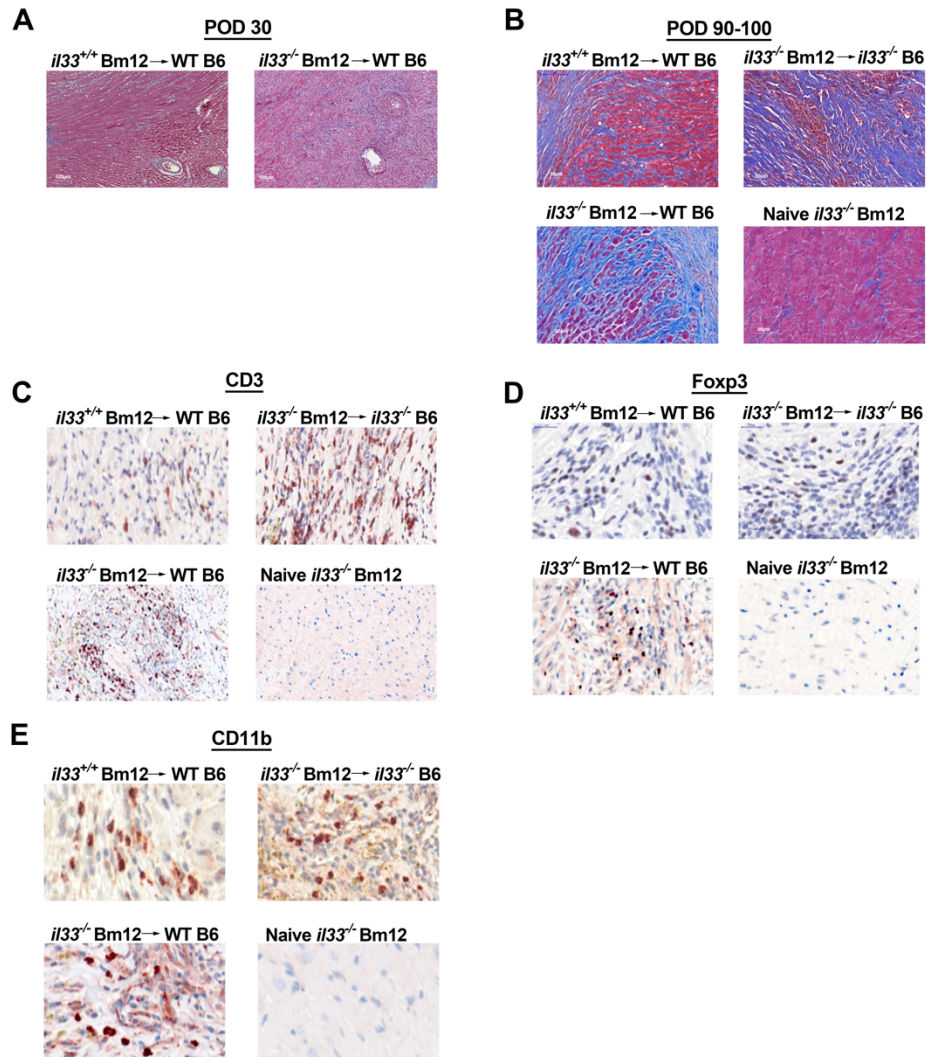
Purified splenic macrophage, Treg, peritoneal macrophages, peritoneal eosinophils, or BMDM RNA was extracted using TRIzol Reagent (Thermo Fisher) per manufacturer instructions and reversed transcribed using the iScript cDNA Synthesis Kit (Biorad). PCR reactions were performed using SYBR Green PCR Master Mix (Applied BioSystems) and amplification completed on an ABI PRISM 7000 Sequence Detection System (Applied BioSystems). Primers for *Nos2* (PPM02928B), *St2/Il1r1* (PPM03546A), and *Gapdh* (PPM02946E) were obtained from Qiagen. Control primers for 18S (Primers for 18s were forward 5' - AACTTTCGATGGTAGTCGCCGT-3' and reverse 5'-TCCTTGATGTGGTAGCCGTTT-3') were obtained from Invitrogen. Data were analyzed using the 2<sup>-ΔΔCT</sup> method (6).

### **Western blotting**

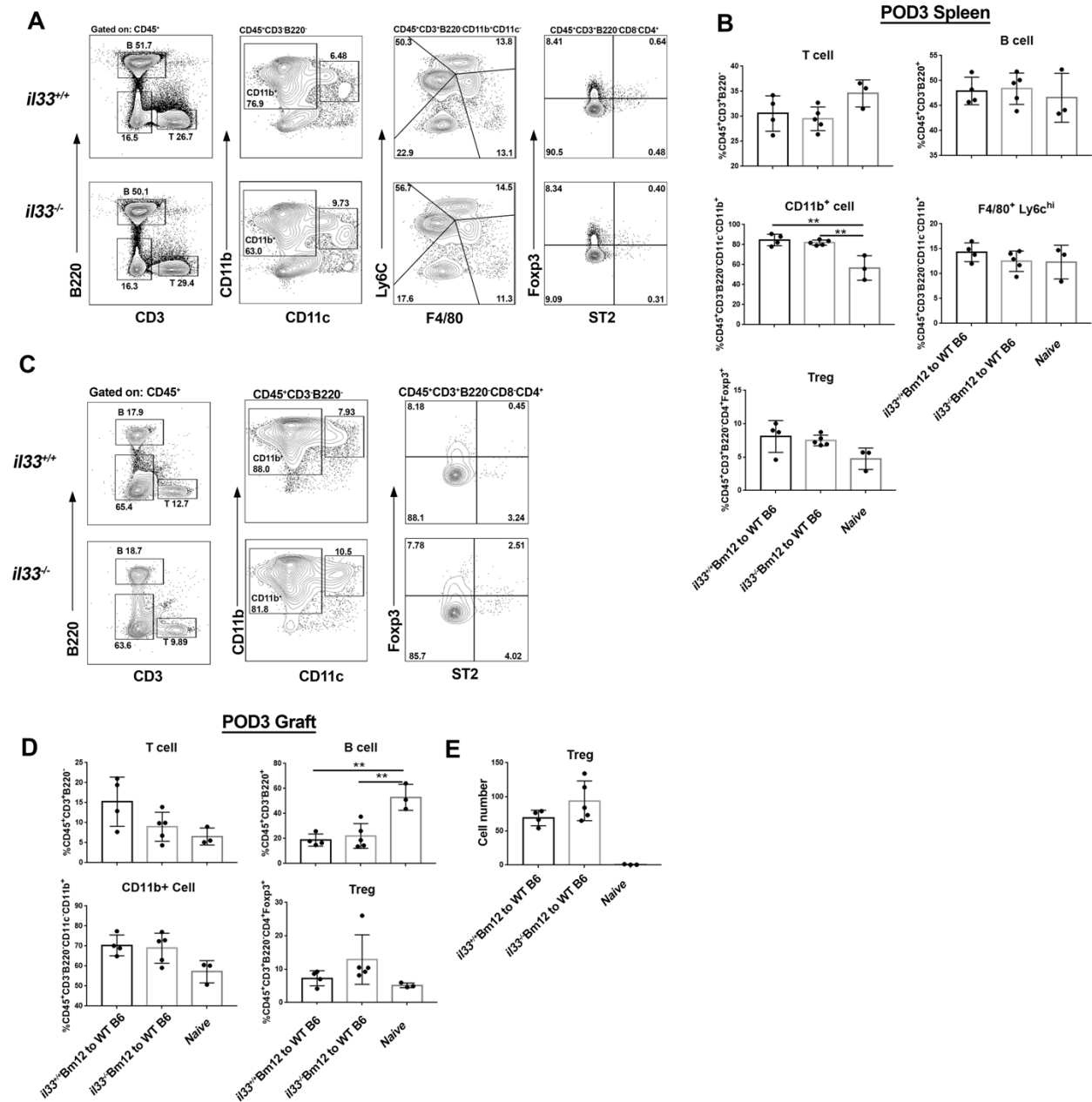
BMDM were generated described in the *Materials and Methods* and cultured at 1-2x10<sup>6</sup> cell per well in a 6-well plate for 15 h in complete media alone (M0) or media supplemented with one or combinations of the following: 1) 20 ng/mL IFN<sub>γ</sub> (Affymetrix eBioscience) and 100 ng/mL LPS (Sigma Aldrich); 2) 20 ng/mL IL-4 (Invitrogen); 3) 20 ng/ml IL-33 (Peprotech). Cells were washed in 1x PBS and lysed in RIPA buffer supplemented with protease inhibitor cocktail. Lysates were kept on ice for 30 minutes, sonicated at 100% amplitude for 3 seconds to shear genomic DNA, and subsequently centrifuged at 12000 rpm for 10 minutes to remove insoluble aggregates. Cell lysates were then separated using SDS-PAGE at 150 V for ~45 minutes in Tris/Glycine buffer on 4-20% ProteanTGX polyacrylamide gels. Separated proteins were then transferred to PVDF membranes for 1h at 300 mAmp fully wet transfer in Tris/Glycine buffer supplemented with 20% methanol. Following transfer, membranes were blocked in 5% BSA in 1X TBST for 1h. Blocking buffer was removed and membranes were incubated with agitation overnight at 4°C in 5% BSA in 1X TBST containing rabbit-anti-iNOS (Invitrogen, PA3-030A) and mouse-anti-β-Actin (Santa Cruz, sc-47778). Following overnight incubation, membranes were washed with TBST, and incubated with agitation for 1h at room temperature in 5% BSA in TBST containing goat-anti-rabbit and goat-anti-mouse HRP-conjugated secondary antibodies (DAKO, P0477, P0448). Membranes were subsequently washed with TBST, incubated for 5 minutes in Clarity ECL chemiluminescent substrate (BioRad), and imaged using ChemiDoc (BioRad) imaging system. Acquired images were analyzed using ImageJ (imagej.nih.gov) and mean pixel density was normalized to β-Actin.



**Supplemental Data Figure 1. Augmented IL-33 is observed in Bm12 allografts.** IL-33<sup>+</sup> Bm12 (*il33<sup>+/+</sup>* Bm12) or IL-33-deficient Bm12 (*il33<sup>-/-</sup>* Bm12) grafts were transplanted into wild type (WT) IL-33 expressing or deficient (*il33<sup>-/-</sup>*) C57BL/6 (B6) recipients (n≥6/group). On post-operation day (POD) 3 or 90-100, grafts were harvested and evaluated by immunofluorescence staining for CD45 (red), Vimentin (white), IL-33 (green) and DAPI (blue). One representative image for each HTx combination group is shown. Bar=20μm, except 5μm in Merge 100x panels.

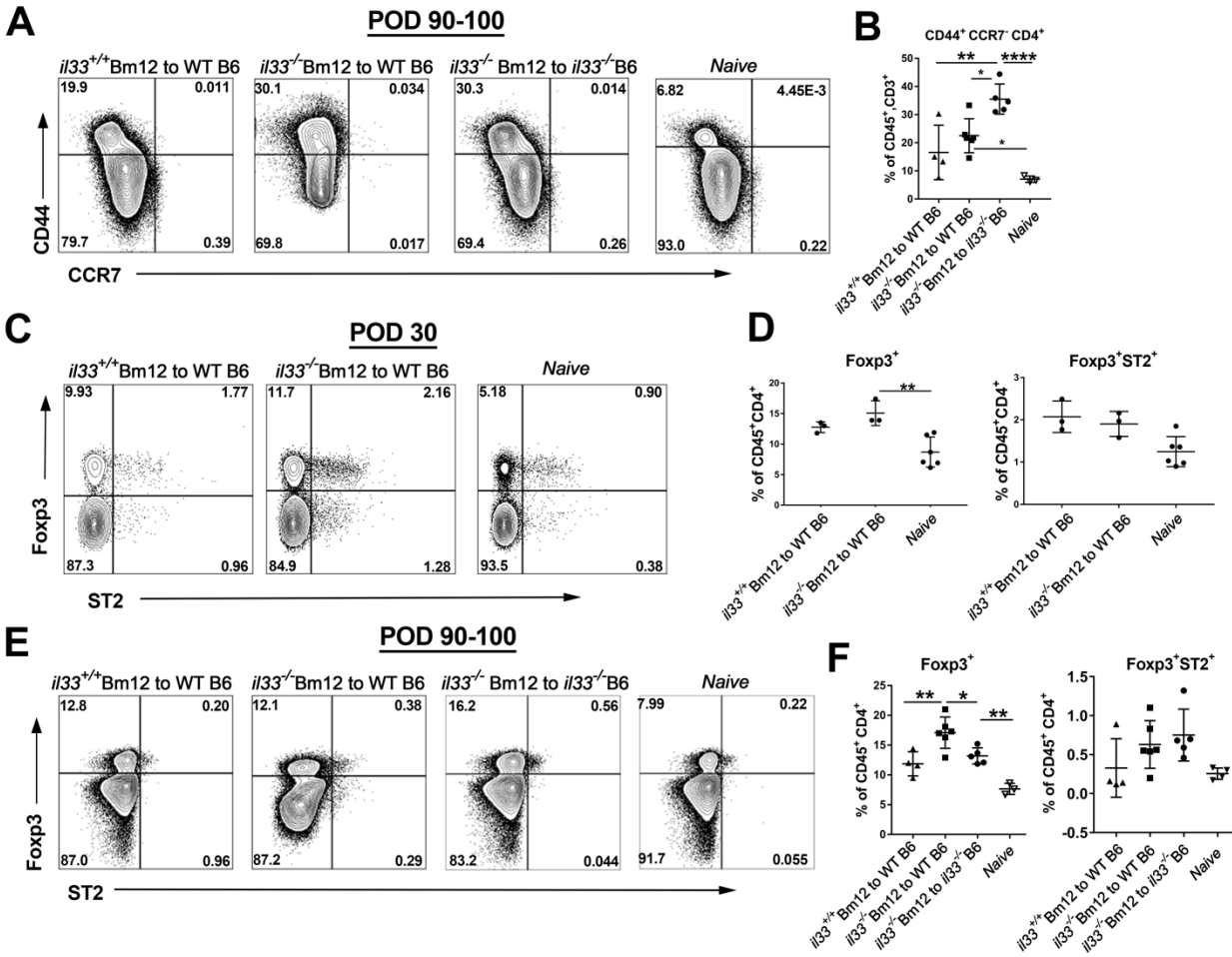


**Supplemental Data Figure 2. Characterization of fibrosis and immune infiltrate in Bm12 cardiac allografts.** **A-E**, IL-33<sup>+</sup> Bm12 (*il33*<sup>+/+</sup> Bm12) or IL-33-deficient Bm12 (*il33*<sup>-/-</sup> Bm12) grafts were transplanted into IL-33-expressing WT or IL-33-deficient (*il33*<sup>-/-</sup>) B6 recipients (n≥6/group). On post-operation (POD) day 30 and 90-100, grafts were harvested and stained with Masson's Trichrome or underwent immunocytochemistry with antibodies to CD3, Foxp3 or CD11b. Representative images from (**A**, **B**) Masson's Trichrome staining and (**C**) CD3, (**D**) Foxp3 or (**E**) CD11b immunocytochemistry are provided. Naïve *il33*<sup>-/-</sup> Bm12 hearts were stained as controls. Bar=50μM.

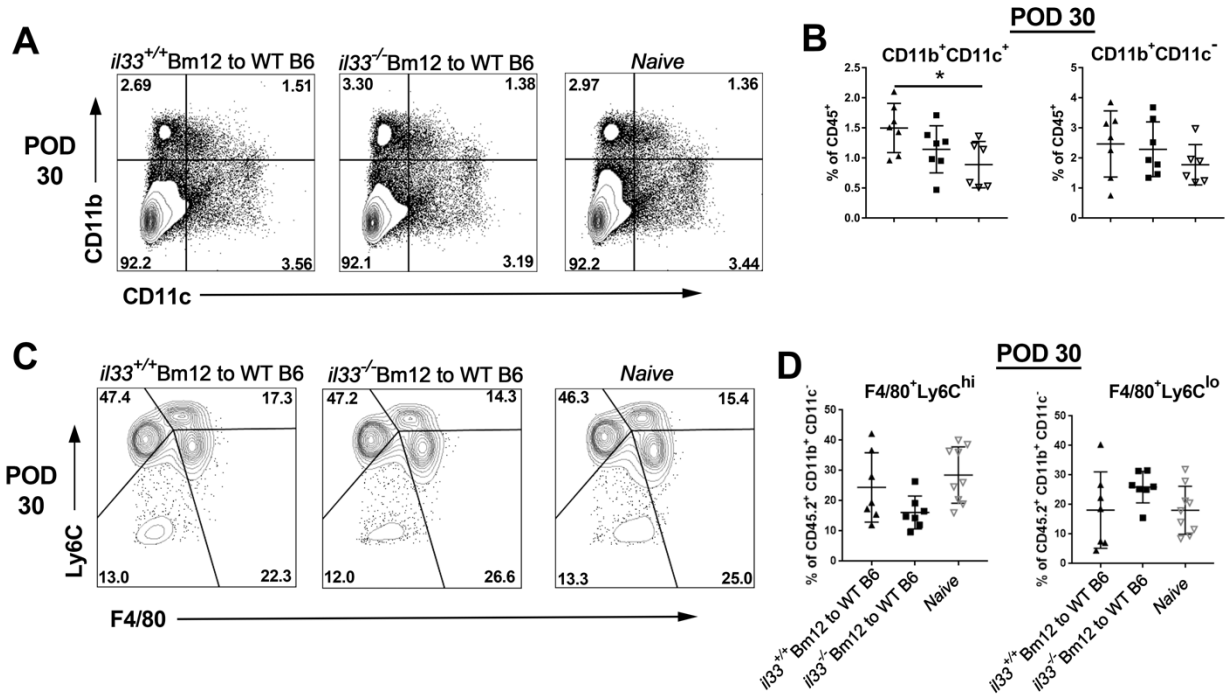


**Supplemental Data Figure 3. No differences observed in WT B6 recipients of *il33*<sup>-/-</sup> or *il33*<sup>+/-</sup> Bm12 heart grafts for overall B cell, T cell, CD11b<sup>+</sup> cell frequency in the spleen or grafts at day 3 POD.**

IL-33-expressing (*il33*<sup>+/-</sup>) or -deficient (*il33*<sup>-/-</sup>) Bm12 grafts were transplanted into WT B6 recipients (n=5-6/group). On POD3, (A, B) splenocytes and (C, D) graft infiltrating leukocytes and were assessed by flow cytometric analysis. Leukocytes from naïve *il33*<sup>+/-</sup> Bm12 mice spleens or hearts were also included as baseline controls (Naive; n=3). (A, C) Representative dot plots for T cell (CD3<sup>+</sup>), B cell (B220<sup>+</sup>) in the CD45<sup>+</sup> gate, CD11b<sup>+</sup> cell in the CD45<sup>+</sup> CD3<sup>-</sup> B220<sup>-</sup> gate and Treg cell in the CD4<sup>+</sup> T cell gate. (B, D) Comparisons of frequencies of T cells, B cells, CD11b cells between indicated groups. (E) Total number of intra-graft Treg. All P values were calculated using a one-way ANOVA. \*P<0.05, \*\*P<0.01.

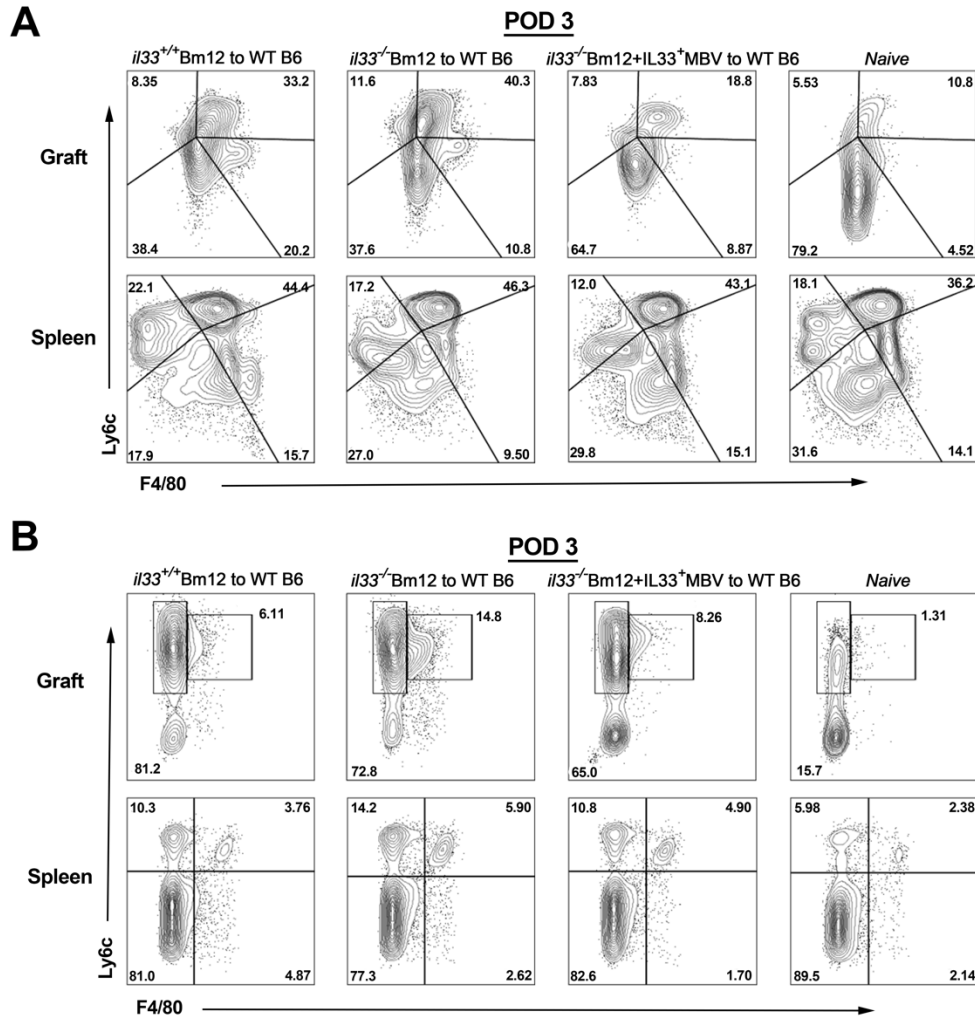


**Supplemental Data Figure 4. The absence of graft IL-33 does not result in systemic changes to T cell subsets after heart transplantation.** IL-33-expressing (*il33*<sup>+/+</sup>) or -deficient (*il33*<sup>-/-</sup>) Bm12 grafts were transplanted into IL-33-expressing WT or IL-33-deficient (*il33*<sup>-/-</sup>) B6 recipients (n=6/group). Recipient splenocytes were then evaluated on POD 30 or 90-100 (n=5-6/group) for changes in T cell populations. Splenocytes from naïve B6 mice were included as controls (n=3-4/group). (A) Representative flow plots for splenic memory CD4<sup>+</sup> T cells are shown for POD 90-100 and (B) comparisons between groups presented as mean±S.D. P values were calculated using ANOVA. \*P<0.05, \*\*P<0.01, \*\*\*\*P<0.001. (C-F) Representative dot plots depicting splenic ST2<sup>+</sup> Treg frequency in the CD45<sup>+</sup> CD4<sup>+</sup> gate at (C) POD 30 and (E) POD 90-100. (D, F) One-way ANOVA was used to compare between groups. \*\*P<0.01, \*P<0.05.



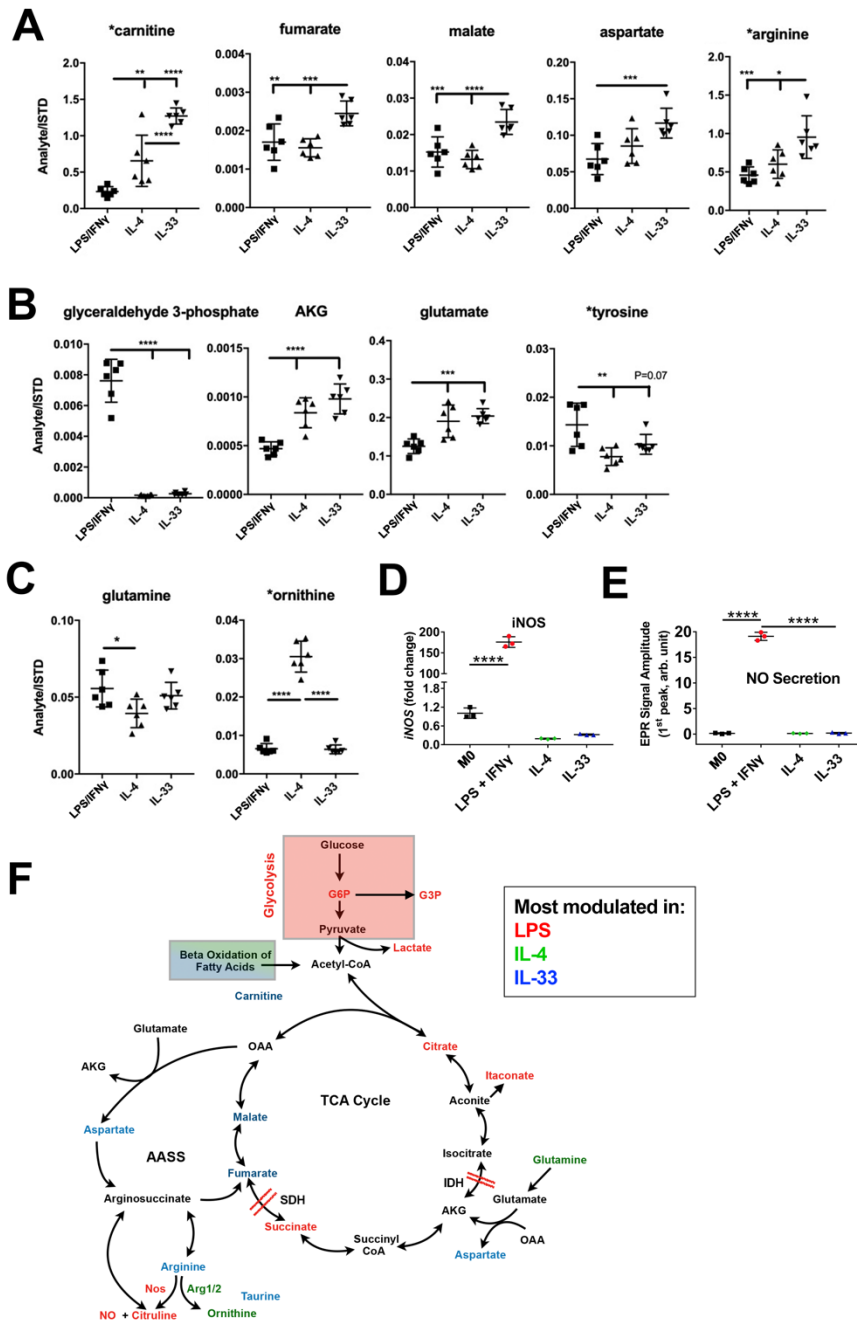
**Supplemental Figure 5. A deficiency of IL-33 in the allograft does not alter the frequency of splenic CD11b<sup>+</sup>CD11c<sup>+</sup> monoDC or macrophage subsets at POD30.**

Splenocytes from IL-33<sup>+</sup> WT B6 recipients of IL-33-expressing (*il33*<sup>+/+</sup>) or -deficient (*il33*<sup>-/-</sup>) Bm12 grafts were evaluated on POD 30 (n=6-7/group) by flow cytometry for changes in monocyte-derived dendritic cell (monoDC) and macrophage subsets. **(A)** Representative dot plots depicting the frequency (%) of CD11b<sup>+</sup>CD11c<sup>+</sup> monoDC in the CD45.2<sup>+</sup>B220<sup>-</sup> cell gate and **(B)** comparisons between groups presented as mean ± S.D. *P* values were calculated using ANOVA. \**P*<0.05. **(C)** Representative dot plot showing splenic macrophage subset characterization within CD45.2<sup>+</sup>B220<sup>-</sup>Ly6C<sup>-</sup>CD11c<sup>+</sup>CD11b<sup>+</sup> the gate **(D)** Comparisons between groups at POD 30 presented as mean ± S.D. *P* values were assessed using ANOVA.



**Supplemental Data Figure 6. Restoring local IL-33 does not alter splenic pro-inflammatory myeloid cells early after transplantation.**

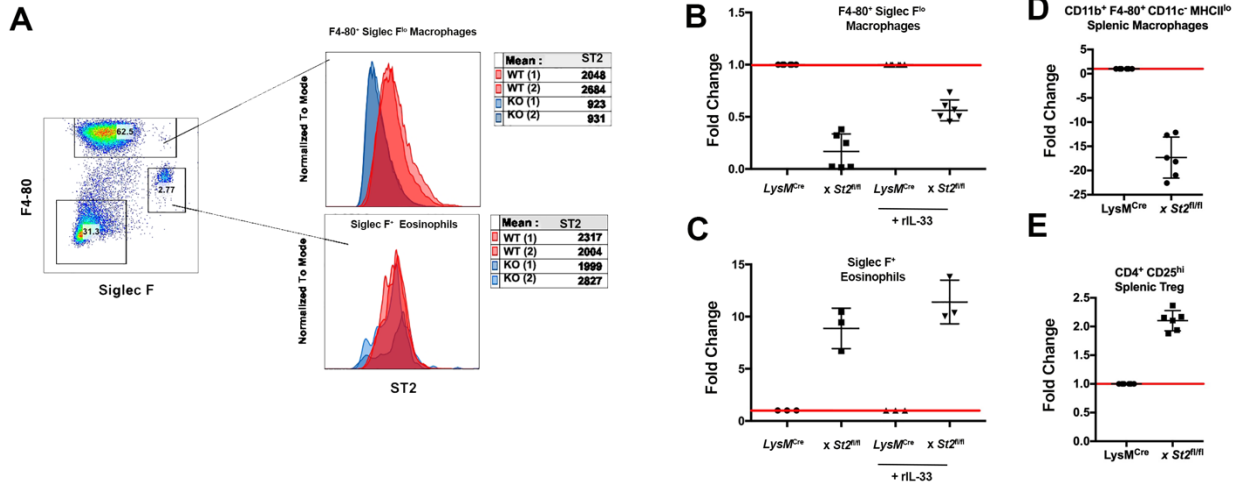
IL-33-expressing (*il33*<sup>+/+</sup>) or -deficient (*il33*<sup>-/-</sup>) Bm12 grafts alone, or IL-33-deficient Bm12 grafts treated with IL-33<sup>+</sup> MBV in Hydrogel (*il33*<sup>-/-</sup> Bm12 + *il33*<sup>+</sup> MBV) were transplanted into WT B6 recipients (n=6/group). On POD3 recipient splenocytes were assessed by flow cytometric analysis. Leukocytes from naïve Bm12 mice hearts were also included as baseline controls (Naïve; n=6). **(A)** Representative dot plots depict macrophage subset frequency in the CD45.2<sup>+</sup>CD19<sup>-</sup>CD49b<sup>-</sup>NK1.1<sup>-</sup>CD90.2<sup>-</sup> Ly6G<sup>-</sup> CD11c<sup>-</sup> CD11b<sup>+</sup> gate. **(B)** Representative dot plots depict monoDC in the CD45.2<sup>+</sup>CD19<sup>-</sup>CD49b<sup>-</sup>NK1.1<sup>-</sup>CD90.2<sup>-</sup>Ly6G<sup>-</sup> gate.



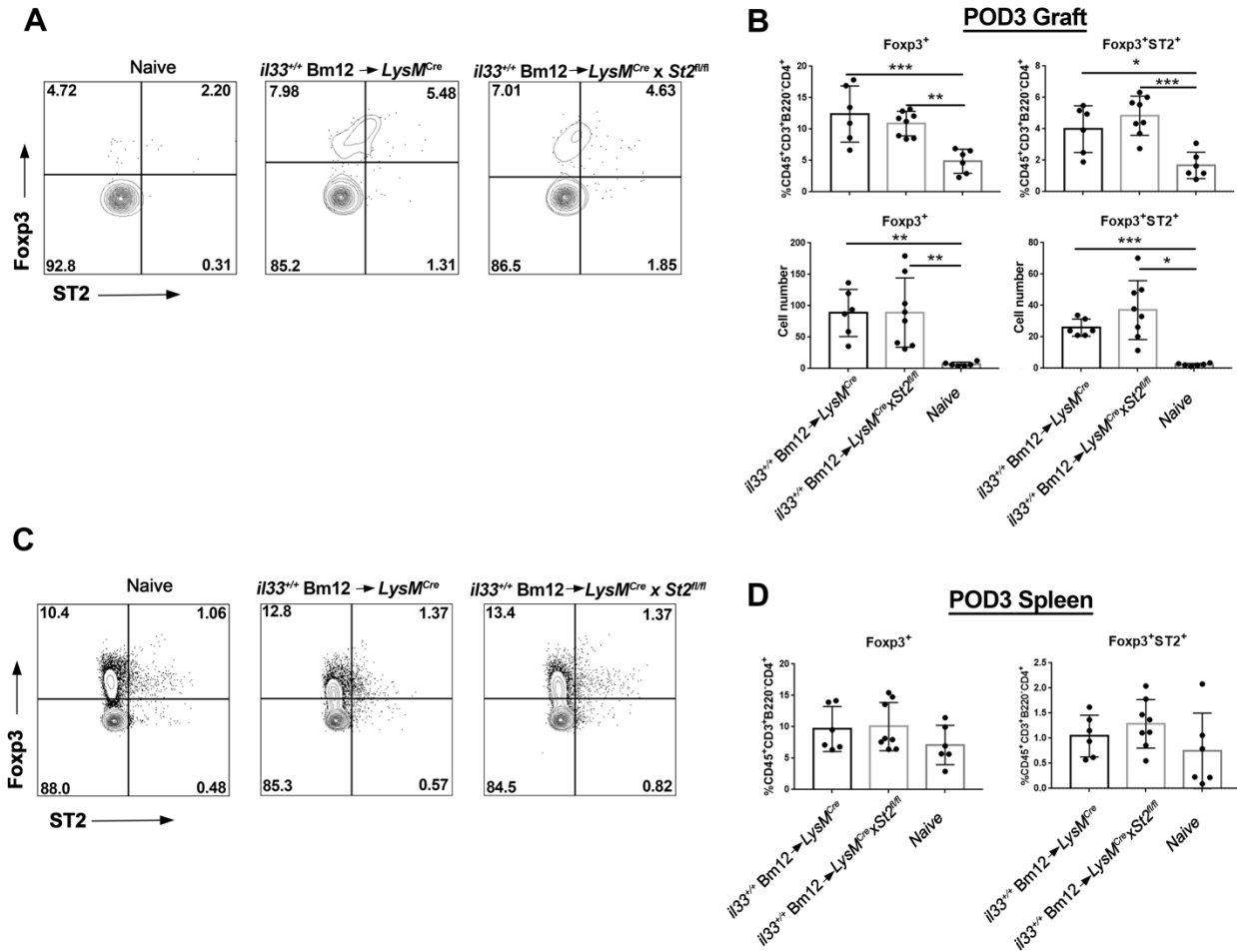
**Supplemental Data Figure 7. Comparison of the metabolic activity of IL-33-stimulated to IL-4 or LPS/IFN $\gamma$  stimulated bone marrow-derived macrophages (BMDM).**

(A-C) Relative concentration (normalized to internal standard and cell number) of TCA metabolites or amino acids\* in macrophage lysates after overnight culture in media with LPS+IFN $\gamma$ , IL-4, or IL-33 determined using LC-HRMS. TCA metabolites or amino acids **A**) increased in IL-33-stimulated BMDM relative to LPS+IFN $\gamma$  or IL-4-stimulated BMDM, **B**) similarly altered in IL-33- and IL-4-stimulated BMDM relative to LPS+IFN $\gamma$ -stimulated BMDM or **C**) uniquely modified in IL-4-stimulated BMDM relative to IL-33- and LPS+IFN $\gamma$ -stimulated BMDM. *P*

values were determined using a one-way ANOVA. \* $P < 0.05$ , \*\* $P < 0.01$ , \*\*\* $P < 0.005$ , \*\*\*\* $P < 0.001$ .  $n = 6$  macrophage samples/group. (D) qRT-PCR measurement of inducible nitric oxide synthase message (*Nos2*) in BMDM RNA. Data are from three independent experiments expressed as mean  $\pm$  SD. One-way ANOVA was used to compare between groups. \*\*\*\* $P < 0.0001$ , \*\*\* $P < 0.001$ , \*\* $P < 0.01$ . (E) EPR measurements of nitric oxide (NO) generation by BMDM was also completed. Data are representative of three independent experiments. \*\*\*\* $P < 0.0001$  calculated using a one-way ANOVA. (F) Schematic summary of differences in metabolic reprogramming between IL-33-stimulated and IL-4- or LPS/IFN $\gamma$ -stimulated BMDC as they relate to aerobic glycolysis, the tricarboxylic acid (TCA) cycle and the aspartate-arginosuccinate shunt (AASS). Metabolites, amino acids, or pathways dominated by each stimulus are indicated by color (IL-33=Blue, IL-4=Green, LPS/IFN $\gamma$ =Red). Red double bars represent NO-induced breaks in the TCA cycle in LPS+IFN $\gamma$ -stimulated BMDM due to NO-inhibition of isocitrate dehydrogenase (IDH) which cause itaconate accumulation (7, 8). This causes a second break in the TCA cycle due to itaconate inhibition of succinate dehydrogenase (SDH), which will increase succinate levels to those triggering pro-inflammatory macrophage activities (9).



**Supplemental Data Figure 8. Effective deletion of ST2 from macrophages of *LysM<sup>Cre</sup>xSt2<sup>fl/fl</sup>* B6 mice.** B6 *LysM<sup>Cre</sup>* alone or *LysM<sup>Cre</sup>xSt2<sup>fl/fl</sup>* were treated via I.P injection of PBS alone or with 0.5-1  $\mu$ g of recombinant IL-33 for 10 days. **(A)** Day 11, peritoneal cells **(A-C)** or splenocytes **(D-E)** were harvested and stained with fluorescent antibodies for flow cytometric assessment or FACS to isolate indicated immune cell populations. **(A)** Flow cytometric assessment of ST2 revealed a decrease in ST2 on peritoneal macrophages, but not eosinophils. Data depicted are from n=2 B6 *LysM<sup>Cre</sup>* (WT) alone or *LysM<sup>Cre</sup>xSt2<sup>fl/fl</sup>* (KO). **(B-E)** Sorted cells assessed by qRT-PCR for ST2 message (*IL1rl1*). Data were analyzed using the  $2^{-\Delta\Delta CT}$  and data are normalized to the WT condition. Data are depicted technical triplicates from 1-2 mice and are representative of multiple experiments.



**Supplemental Data Figure 9. Loss of macrophage ST2 does not alter frequency of ST2<sup>+</sup> Treg in the spleen or graft.**

IL-33-expressing (*i133<sup>+/+</sup>*) Bm12 grafts were transplanted into B6 *LysM<sup>Cre</sup>* or *LysM<sup>Cre</sup>*x*St2<sup>fl/fl</sup>* recipients (n=6-8/group). On POD3, graft infiltrating leukocytes (**A, B**) and splenocytes (**C, D**) were assessed by flow cytometric analysis. Leukocytes from naïve Bm12 mice hearts were also included as baseline controls (Naive; n=6). (**A, C**) Representative dot plots for Treg cell, ST2<sup>+</sup>Treg cell in the CD45<sup>+</sup>CD3<sup>+</sup>B220<sup>-</sup>CD8<sup>-</sup>CD4<sup>+</sup> gate. (**B, D**) Scatter graphs depict individual mouse frequency of Treg cell, ST2<sup>+</sup>Treg cell in the CD45<sup>+</sup>CD3<sup>+</sup>B220<sup>-</sup>CD8<sup>-</sup>CD4<sup>+</sup> gated population and group mean±S.D. All *P* values were calculated using a one-way ANOVA. \**P*<0.05, \*\**P*<0.01, \*\*\**P*<0.005, \*\*\*\**P*<0.001.

## Supplemental References:

1. Turnquist HR, Zhao Z, Rosborough BR, Liu Q, Castellaneta A, Isse K, et al. IL-33 Expands Suppressive CD11b<sup>+</sup> Gr-1<sup>int</sup> and Regulatory T Cells, including ST2L<sup>+</sup> Foxp3<sup>+</sup> Cells, and Mediates Regulatory T Cell-Dependent Promotion of Cardiac Allograft Survival. *Journal of Immunology*. 2011;187(9):4598-610.
2. Everts B, Amiel E, van der Windt GJ, Freitas TC, Chott R, Yarasheski KE, et al. Commitment to glycolysis sustains survival of NO-producing inflammatory dendritic cells. *Blood*. 2012;120(7):1422-31.
3. Zhu Y, Matsumura Y, Velayutham M, Foley LM, Hitchens TK, and Wagner WR. Reactive oxygen species scavenging with a biodegradable, thermally responsive hydrogel compatible with soft tissue injection. *Biomaterials*. 2018;177:98-112.
4. Cardounel AJ, Cui H, Samouilov A, Johnson W, Kearns P, Tsai AL, et al. Evidence for the pathophysiological role of endogenous methylarginines in regulation of endothelial NO production and vascular function. *J Biol Chem*. 2007;282(2):879-87.
5. Xia Y, Cardounel AJ, Vanin AF, and Zweier JL. Electron paramagnetic resonance spectroscopy with N-methyl-D-glucamine dithiocarbamate iron complexes distinguishes nitric oxide and nitroxyl anion in a redox-dependent manner: applications in identifying nitrogen monoxide products from nitric oxide synthase. *Free Radic Biol Med*. 2000;29(8):793-7.
6. Livak KJ, and Schmittgen TD. Analysis of relative gene expression data using real-time quantitative PCR and the 2<sup>-</sup>( $\Delta\Delta C_T$ ) Method. *Methods*. 2001;25(4):402-8.
7. Van den Bossche J, Baardman J, Otto NA, van der Velden S, Neele AE, van den Berg SM, et al. Mitochondrial Dysfunction Prevents Repolarization of Inflammatory Macrophages. *Cell Rep*. 2016;17(3):684-96.
8. Bailey JD, Diotallevi M, Nicol T, McNeill E, Shaw A, Chuaiphichai S, et al. Nitric Oxide Modulates Metabolic Remodeling in Inflammatory Macrophages through TCA Cycle Regulation and Itaconate Accumulation. *Cell Rep*. 2019;28(1):218-30 e7.
9. Tannahill GM, Curtis AM, Adamik J, Palsson-McDermott EM, McGettrick AF, Goel G, et al. Succinate is an inflammatory signal that induces IL-1 $\beta$  through HIF-1 $\alpha$ . *Nature*. 2013;496(7444):238-42.